Pol. J. Environ. Stud. Vol. XX, No. X (XXXX), 1-12
DOI: *10.15244/pjoes/215764* ONLINE PUBLICATION DATE: 2026-02-18

Original Research

Physicochemical Characteristics, Pyrolysis Behavior, and Kinetics of Packaging Solid Waste from the Tobacco Logistics Industry

Weichang Gao[1], Xinjian Li[2], Xiaoqi Lin[2], Taoze Liu[3, 4]*, Guangneng Zeng[3], Zhanghong Wang[3, 4°]**

[1]Upland Flue-Cured Tobacco Quality & Ecology Key Laboratory of CNTC, Guizhou Academy of Tobacco Science, Guiyang 550081, PR China
[2]Qiannan Prefecture Company of Guizhou Tobacco Company, Duyun 558000, PR China
[3]College of Eco-Environmental Engineering, Guizhou Minzu University, Guiyang 550025, PR China
[4]Engineering Research Center of Green and Low-carbon Technology for Plastic Application, Guizhou Minzu University, Guiyang 550025, PR China

Received: 26 September 2025
Accepted: 17 December 2025

Abstract

To promote the green development of the tobacco logistics industry and realize resource utilization of its solid packaging waste, this study investigated plastic wrapping film (polyethylene, PE), logistics cardboard boxes (LCB), logistics wood strips (LWS), and cigarette packaging paper (CPP) as representative materials. Comprehensive analyses were conducted on their composition, surface functional groups, morphology, crystal phases, chemical bonds, and pyrolysis behaviors. Furthermore, the co-pyrolysis interactions and kinetic parameters of PE blended with LCB, LWS, or CPP were studied. The results showed that PE is mainly composed of C, H, and trace O, with C-H and -OH as dominant surface functional groups. In contrast, LCB, LWS, and CPP are rich in C, H, O, N, and S, with major surface functional groups of C=O, -C-O, C-H, and -OH, and contain substantial mineral particles or additives. PE displays high thermal stability, decomposes within a narrow temperature range (407~485°C), and produces negligible solid residue after pyrolysis. During co-pyrolysis, there are strong interactions between PE and LCB, LWS, or CPP. Notably, the presence of minerals or additives in LCB can greatly mitigate the negative effects of PE softening, shifting the pyrolysis temperature of both LCB and PE to lower regions and reducing their activation energies to 11.43 and 16.53 kJ/mol, respectively. The study demonstrates that co-pyrolysis is a feasible approach for the resource utilization of solid waste from the tobacco logistics industry.

Keywords: tobacco logistics industry, packaging solid waste, plastic wrapping film, physicochemical properties, pyrolysis

*e-mail: liutaoze2025@163.com
**e-mail: z.wang2021@hotmail.com
°ORCID iD: 0000-0002-0334-033X

Introduction

With the ongoing advancement of global green and low-carbon development, China's tobacco industry is facing unprecedented pressure to transform. As a critical component of the national economy, the tobacco industry encompasses tobacco cultivation, research and development, processing, sales, and associated logistics, playing a vital role in promoting employment, stimulating local economies, and generating tax revenue [1]. However, alongside its rapid growth, the tobacco industry confronts environmental challenges such as high energy consumption, large pollutant emissions, and substantial carbon footprints, which have become bottlenecks restricting the industry's sustainable development [2]. In response to the national call for energy conservation, emission reduction, and green development, accelerating the green and low-carbon transformation of the tobacco industry, especially by strengthening green management and resource recycling in the logistics sector, has become an urgent and significant issue.

As a key supporting link within the tobacco industrial chain, the logistics sector plays a central role in enhancing cigarette circulation efficiency, ensuring product quality, and reducing operational costs. In recent years, with advancing automation and informatization, the management and service levels of tobacco logistics have become increasingly standardized and modernized [3]. In the selection of packaging materials and logistics operations, to reduce resource consumption and environmental burden, companies are actively promoting the adoption of degradable and recyclable green logistics materials, such as high-strength plastic wrapping films and recyclable cardboard boxes. However, after multiple cycles of use or prolonged service life, packaging materials inevitably undergo aging and damage, or may incur losses during handling and storage, resulting in a portion of materials eventually being discarded as solid waste. With the continued expansion of the tobacco logistics sector, the generation and management of packaging solid waste is becoming increasingly challenging. Finding efficient and environmentally friendly ways to dispose of this organic solid waste has thus become one of the critical issues limiting the green development of the industry.

At present, the dominant types of solid waste in the tobacco logistics industry include plastic wrapping films, cardboard packaging boxes, wooden logistics strips, and cigarette packaging paper [3]. This waste is compositionally complex and represents typical organic solid waste [4]. Their common characteristics include low bulk density, high porosity, low energy density, and generally low recycling value. Traditional disposal methods, such as landfill or direct incineration, not only occupy land resources but are also prone to causing secondary environmental pollution [5]. Therefore, there is an urgent need to explore new, efficient, low-carbon, and resource-oriented pathways for their management and utilization. Among them, pyrolysis technology demonstrates huge application potential in organic solid waste management due to its ability to rapidly reduce waste volume and produce biochar, syngas, bio-oil, and other high value-added chemicals [6, 7]. Particularly, under the targets of "carbon peaking and carbon neutrality", pyrolysis is expected to achieve the integrated goals of clean and harmless disposal and resource recycling of solid waste.

In recent years, as pyrolysis equipment and processes have continued to innovate, co-pyrolysis of organic solid waste blends has attracted increasing attention. Co-pyrolysis refers to the synergistic thermal treatment of two or more types of organic solid waste with distinct properties, blended at appropriate ratios. This process not only accommodates the disposal needs of multiple waste streams but may also, via synergistic thermochemical reactions between feedstocks, improve the quality and yield of target products [8, 9]. In practice, however, the effectiveness of co-pyrolysis is affected by the physicochemical properties of each waste component (e.g., organic content, fiber-to-resin ratio), their individual pyrolysis behaviors, and mutual interactions during thermal decomposition. Variations in feedstock characteristics and process conditions inevitably influence the types, yields, and distributions of pyrolytic products [10-12]. Therefore, systematically clarifying the physicochemical properties, as well as the individual and co-pyrolysis behaviors and mechanisms of typical organic solid waste from the tobacco logistics industry, constitutes the theoretical and technical foundation for efficient resource utilization.

Herein, this study takes representative solid packaging waste from the commercial cigarette logistics sector, including plastic wrapping films (polyethylene, PE), discarded logistics cardboard (LCB), discarded logistics wood strips (LWS), and discarded cigarette packaging paper (CPP), as research objects. According to our field survey, PE, LCB, LWS, and CPP represent the major types of solid waste produced in the commercial cigarette logistics sector of Guizhou Province. First, their physicochemical properties were systematically analyzed, including material composition, surface morphology (SEM), surface functional groups (FT-IR), and crystalline structure (XRD). Then, thermogravimetric analysis (TGA) was used to explore the pyrolysis processes, kinetic behaviors, and interaction mechanisms of both single components and blended waste (see Fig. 1). Finally, pyrolysis kinetic parameters were quantitatively employed to reveal the synergistic mechanisms inherent in co-pyrolysis, providing theoretical support and technological reference for efficient and green resource utilization of solid waste in the tobacco logistics industry. This research supports the low-carbon transformation of the tobacco industry and holds significant practical value for the reduction, harmless treatment, and resource utilization of packaging solid waste.

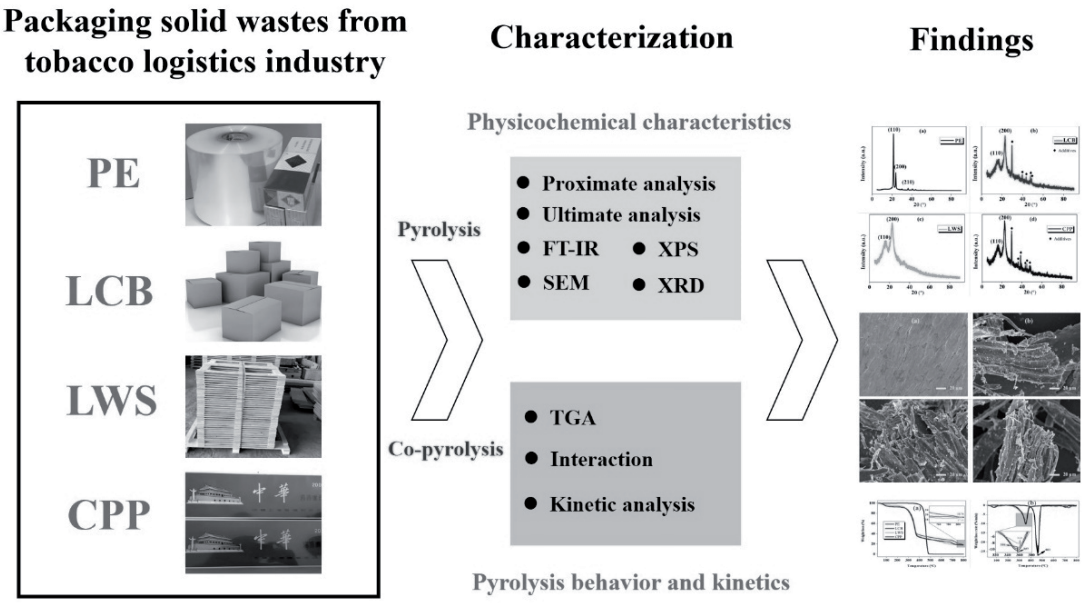

Fig. 1. Illustration summarizing this study.

Materials and Methods

Raw Materials

Tobacco logistics waste, including plastic wrapping film (polyethylene, PE), discarded logistics cardboard (LCB), discarded logistics wood strips (LWS), and discarded cigarette packaging paper (CPP), were collected from a tobacco commercial logistics center in Guizhou Province, China. After manual removal of extraneous materials, the collected samples were oven-dried and ground for subsequent analyses.

Physicochemical Property Analysis

Proximate analysis of the samples, including ash content, moisture, fixed carbon, and volatile matter, was performed using a horizontal tube furnace (OTL 1200, Nanjing Nanda, Nanjing, China). The inorganic elemental composition (C, H, N, and S) of the samples was determined using an elemental analyzer (EA112, Thermo Finnigan, San Jose, CA, USA). The concentration of oxygen was calculated by difference. A Fourier-transform infrared spectrometer (Nicolet 6700, Thermo Fisher Scientific, USA) was employed to identify the surface functional groups of the samples. The micro-morphology was examined using a scanning electron microscope (Inspect F50, FEI, USA). The crystalline structure of the samples was analyzed by powder X-ray diffraction (XRD, SmartLAB 3, Rigaku, Japan). X-ray photoelectron spectroscopy (XPS, Thermo-ESCALAB 250, USA) was used to examine the chemical composition and bonding states. Thermogravimetric analysis (TGA, TG209F3, Netzsch, Germany) was conducted to evaluate mass loss behaviors during pyrolysis, both for individual and blended samples. For blended samples, PE was mixed with CPP, LCB, or LWS at a mass ratio of 5:1~1:5 and homogenized by grinding prior to the experiments.

Results and Discussion

Physicochemical Properties

Proximate Analysis and Ultimate Analysis

As shown in Table 1, the proximate and elemental compositions of PE differ markedly from those of biomass-derived solid waste such as LCB, LWS, and CPP. First, PE exhibits a relatively high volatile matter content (>99.15%) and comparatively low ash, moisture, and fixed carbon contents. This ensures that PE undergoes complete decomposition during thermal conversion, leaving no solid residue, a phenomenon extensively reported in previous research [11, 13]. In contrast, LCB, LWS, and CPP have significantly lower volatile matter and relatively high fixed carbon contents (10.76%~27.67%). It has been reported that for organic solid waste, the yield of residual char (biochar) from pyrolysis is closely related to its intrinsic fixed carbon content [12]. Elemental analysis indicates that PE is primarily composed of C and H, contains negligible N and S, but does have a small amount of O. The presence of O may be related to aging processes or moisture adsorption during PE usage [12]. During the aging process, such as thermal shrinkage or mechanical stretching, partial oxidation may occur, introducing oxygen-containing groups into the polymer structure. In addition, the H/C ratio of PE is 0.16, suggesting its potential as a high-quality hydrogen donor that can facilitate further decomposition and deoxygenation

Table 1. Physicochemical properties of packaging solid waste in the tobacco commercial cigarette logistics industry.

	Proximate analysis				Ultimate analysis					H/C	O/C
	Ash	Moisture	FC[a]	VM[b]	C	H	O	N	S		
	(%)				(%)						
PE	0.21	0.13	0.49	99.15	84.39	13.58	1.63	0	0	0.16	0.02
LCB	3.45	2.43	14.34	79.78	44.78	4.76	41.37	0.65	0.23	0.11	0.92
LWS	1.78	1.56	27.67	68.79	43.58	5.20	42.90	0.85	0.36	0.12	0.98
CPP	2.56	1.06	10.76	85.86	43.58	4.46	41.33	1.25	0.63	0.10	0.95

Note: a and b are fixed carbon and volatile matter, respectively.

of other materials during co-pyrolysis reactions [14]. In comparison, LCB, LWS, and CPP exhibit considerably more complex elemental compositions, characterized by markedly elevated O contents, yielding O/C ratios in the range of 0.92~0.98. Additionally, appreciable amounts of N and S are also present in these materials.

Surface Functional Groups

The FT-IR spectra (Fig. 2) show that PE exhibits the typical characteristic functional groups of polyethylene, with absorption bands at 2920 and 2850 cm^{-1} corresponding to the asymmetric and symmetric C-H stretching vibrations of $-CH_2-$, respectively. The absorption at 1475 cm^{-1} is attributed to the bending vibration of C-H in $-CH_2-$, while the band at 720 cm^{-1} is ascribed to the rocking vibration of C-H in $-CH_2-$. In addition, a broad absorption band for -OH stretching vibrations is observed in the range of 3450~3320 cm^{-1}, which may be attributed to oxidative aging of PE during use [15]. These observations are consistent with the results presented in Table 1. In contrast, the functional group vibrations in LCB, LWS, and CPP are relatively weak, dominated by absorption peaks associated with oxygen-containing functional groups, such as -OH stretching at 3450~3320 cm^{-1}, C=O stretching at 1645~1600 cm^{-1}, and -C-O stretching at 1100-1000 cm^{-1}. This is in line with the higher O content found in LCB, LWS, and CPP (see Table 1). According to previous studies, the relatively weak (broad and blunt) surface functional group peaks observed in biomass-derived solid waste can be attributed to the complex variety of functional groups present, as well as mutual interference, overlap, and masking effects among these groups [16].

Surface Morphology Analysis

As shown in Fig. 3, the surface of PE is relatively smooth and flat (Fig. 3a)), with no obvious particulate or porous structures observed. In contrast, LCB, LWS, and CPP display irregular bundle-like structures, primarily arising from their intrinsic fibrous components, while the irregular morphology is largely the result of distortions introduced during mechanical comminution. This interpretation is corroborated by the abundant fibrous debris evident on the surfaces of LCB, LWS, and CPP. In addition, a large number of fine particulates

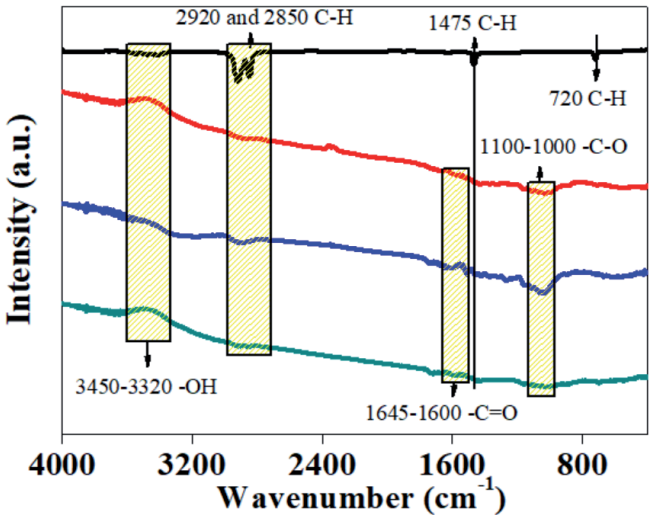

Fig. 2. FT-IR spectra of packaging solid waste in the tobacco commercial cigarette logistics industry.

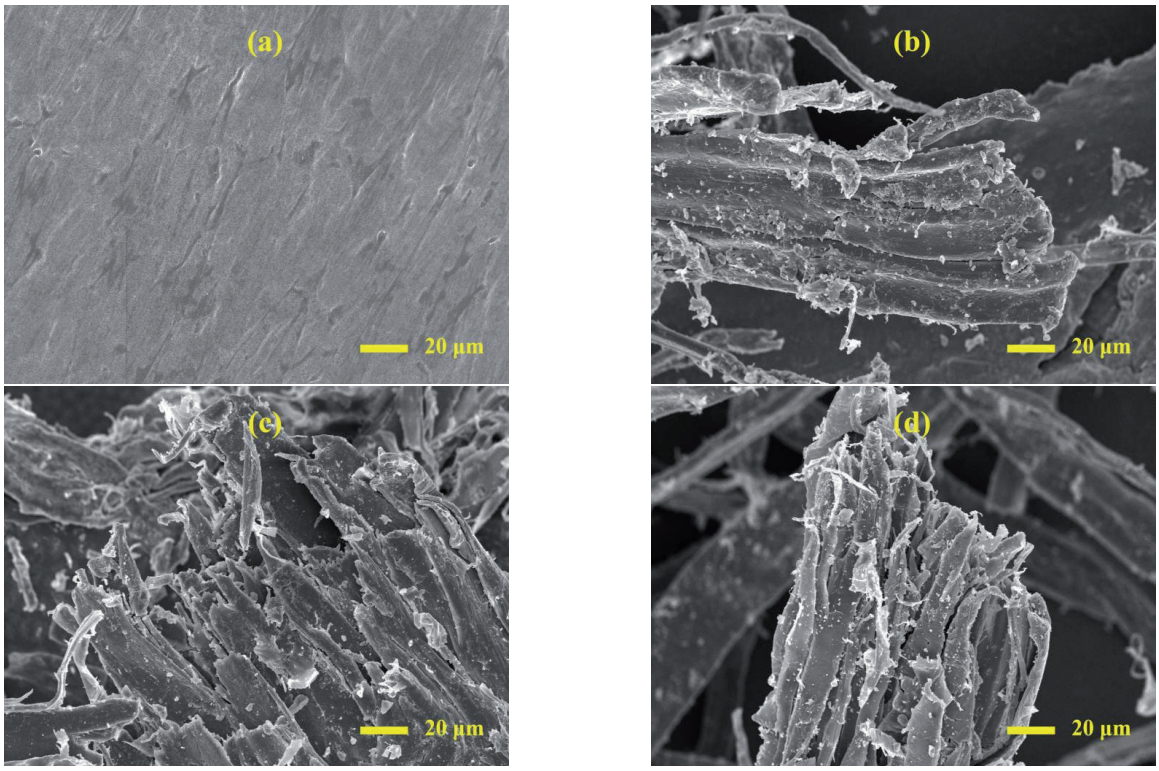

Fig. 3. SEM images of packaging solid waste in the tobacco commercial cigarette logistics industry; a) PE, b) LCB, c) LWS, and d) CPP.

are present on the surfaces of these materials, which can be attributed to the presence of mineral particles or additives [17]. As shown in Table 1, the ash content of LCB, LWS, and CPP is approximately 1.78~3.45%, consistent with the findings of the morphological analysis.

XRD Analysis

As shown in Fig. 4, the XRD pattern of PE exhibits characteristic diffraction peaks at 2θ values of approximately 21.5°, 23.8°, and 36.5°, which correspond to the (110), (200), and (210) crystal planes, respectively. These features indicate a typical orthorhombic crystalline structure, consistent with the reported crystallization behavior of polyethylene in the literature [18]. In contrast, LWS exhibits characteristic diffraction peaks at around 16.5° and 22.5° (2θ), corresponding to the (110) and (200) planes, respectively, along with a broad amorphous diffraction band. This pattern reveals the coexistence of crystalline and amorphous regions in LWS, which is associated with the presence of cellulose crystallites and the amorphous domains contributed by lignin and hemicellulose [19]. Similarly, LCB and CPP display comparable diffraction peaks, reflecting their primary composition of biomass-derived cellulose. In addition, multiple diffraction peaks attributable to additives can be observed in the XRD patterns of LCB and CPP, consistent with the results from SEM analysis.

XPS Analysis

XPS analysis reveals that PE primarily contains C and O, whereas LCB, LWS, and CPP are composed of C, O, N, and S (see Table 2), which is largely consistent with the results presented in Table 1. Notably, the C contents determined by XPS in Table 2 are significantly higher than those obtained by elemental analysis in Table 1; this discrepancy is attributable to the absence of H detection in XPS. Since hydrogen atoms possess only a 1s electron with extremely low binding energy, the resulting photoelectrons have insufficient energy and are readily scattered or absorbed, rendering conventional XPS ineffective for their accurate collection and analysis. Similar trends have also been reported in previous studies, where higher carbon contents were observed in XPS results due to the exclusion of hydrogen detection [13, 20].

The XPS survey spectrum of PE confirms the presence of C and O, corresponding to the C1s and O1s peaks, respectively (Fig. 5a)). Peak deconvolution reveals that the high-resolution C1s spectrum of PE is mainly composed of three characteristic peaks at 284.0, 284.8, and 285.9 eV, which can be assigned to C-C, C-C/C-H, and C-O bonds, respectively (Fig. 5b)). The presence of C-O is primarily attributed to mild oxidative aging on the PE surface, resulting in the formation of alcohols, ethers, and similar functional groups. The high-resolution O1s spectrum further confirms the existence of C-O bonds and degradation of the -CH_2- main chain. By contrast, in addition to C1s and O1s peaks, the XPS

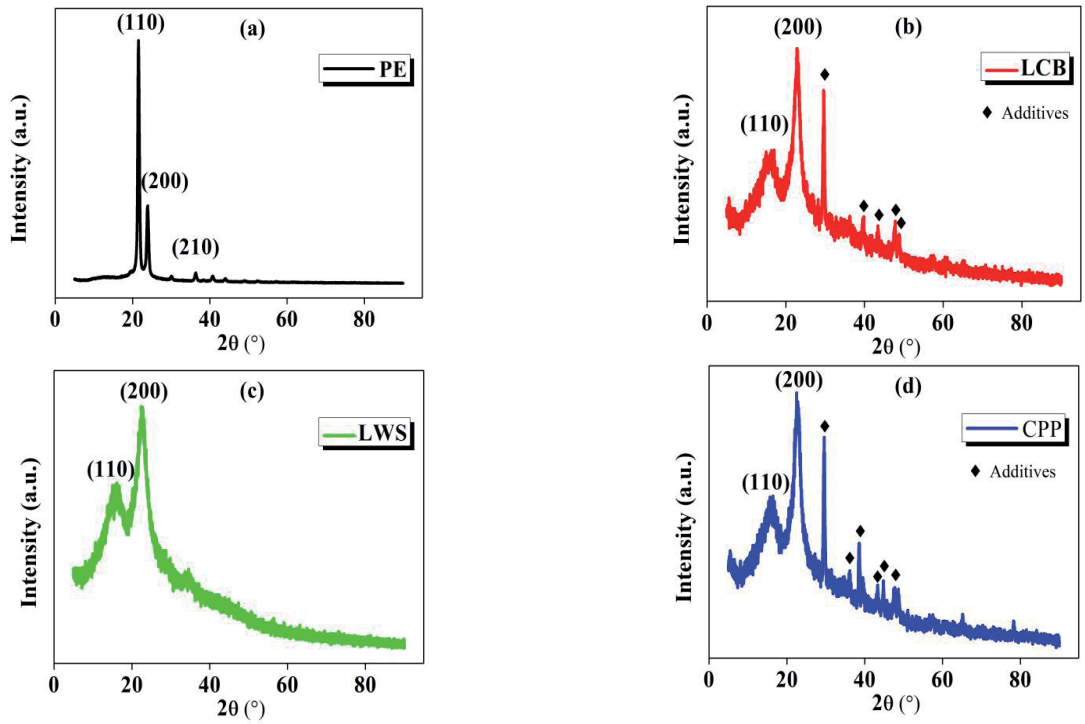

Fig. 4. XRD patterns of packaging solid waste in the tobacco commercial cigarette logistics industry; a) PE, b) LCB, c) LWS, and d) CPP.

Table 2. Elemental composition determined by XPS analysis.

	C (%)	O (%)	N (%)	S (%)
PE	99.15	0.85	-[a]	-
LCB	64.40	33.93	1.47	0.19
LWS	72.2	26.31	1.36	0.13
CPP	65.13	33.75	0.79	0.32

Note: a below the determination limit.

survey spectra of LCB, LWS, and CPP also show N1s and S2p peaks (Fig. 5f), k), and p)). High-resolution C1s spectra of LCB reveal a main contribution at 284.7 eV assigned to the C-C bonds from the cellulose backbone, 286.5 eV for C-O bonds in alcohols, ethers, and hemicellulose, and 288.2 eV for C=O bonds in carbonyl and carboxyl groups (Fig. 5g)). The O1s spectrum indicates two typical chemical states of oxygen: the C=O bond at 530.4 eV attributed to carbonyl or carboxyl groups, and the C-O bond at 532.0 eV. Trace nitrogen-containing organics in LCB are evidenced by the N1s peak at 399.1 eV, corresponding to C=N-C, which most likely originates from nitrogen-containing heterocycles introduced during ink application, additives, or fiber modification in papermaking. The S2p spectrum of LCB exhibits a peak at 167.8 eV assigned to C-S-C, indicating the presence of minor sulfur species, likely associated with papermaking or printing additives. Similarly, LWS and CPP present chemical bonds and functional groups analogous to those found in LCB, with the main differences lying in their relative contents.

Pyrolysis Behavior

Individual Components

The TG curve demonstrates that PE exhibits relatively high thermal stability, with less than 1% mass loss observed at pyrolysis temperatures below 407°C (Fig. 6a)). When the temperature exceeds 407°C, PE undergoes rapid decomposition and achieves complete conversion within a relatively narrow temperature range (407~485°C), leaving no solid residue. The DTG curve reveals that the maximum rate of mass loss for PE occurs at approximately 461°C, with a peak value of -26.15 %/min (Fig. 6b)). Detailed pyrolysis parameters are provided in Table 3.

In contrast, the pyrolysis process of LCB, LWS, and CPP can be broadly divided into four stages: dehydration, pyrolysis preparation, main pyrolysis, and carbonization (Fig. 6a)) [21]. As indicated by the FT-IR results, LCB, LWS, and CPP are rich in oxygen-

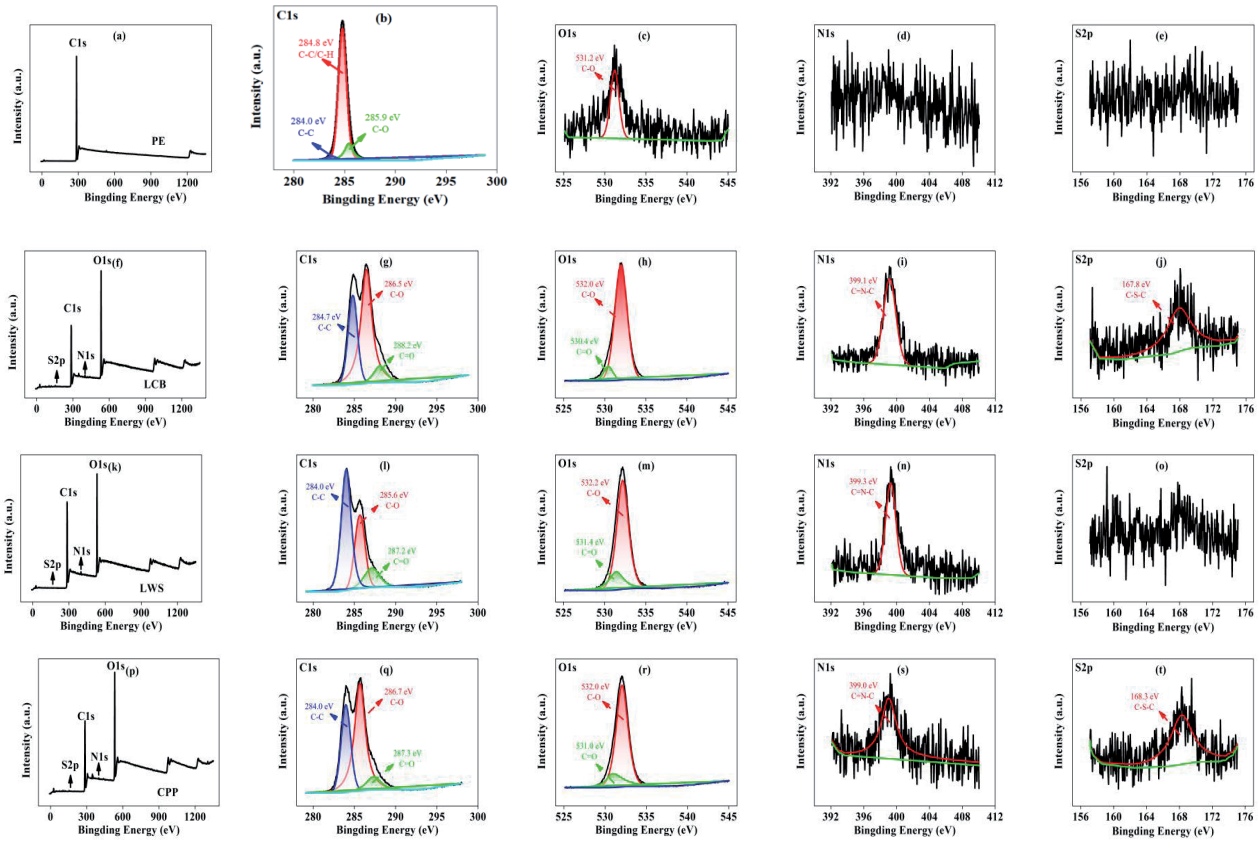

Fig. 5. XPS spectra of packaging solid waste in the tobacco commercial cigarette logistics industry; (a-e) PE; (f-j) LCB; (k-o) LWS, and (p-t) CPP.

containing functional groups, which impart relatively high hydrophilicity and enable the retention of free moisture from the environment. This fraction of water is rapidly released from the biomass near the boiling point of water. As the pyrolysis temperature increases further, no significant mass loss is observed; however, glass transition occurs in the internal structure, preparing the material for rapid decomposition during the main pyrolysis stage. When the temperature approaches approximately 270°C, the biomass undergoes rapid decomposition and substantial mass loss (see Table 3). The pyrolysis process gradually slows down after around 370°C. According to the literature, the decomposition temperatures for hemicellulose, cellulose, and lignin

Table 3. Pyrolysis/Co-pyrolysis parameters of packaging solid waste in the tobacco commercial cigarette logistics industry.

	Pyrolysis range (°C)				Maximum weight loss rate (°C)/min		Peak temperature (°C)	
	T_{i1} [a]	T_{fi} [b]	T_{i2} [c]	T_{f2} [d]	$(dm1/dt)_{max}$ [e]	$(dm1/dt)_{max}$ [f]	T_{p1} [g]	T_{p1} [h]
PE			407	485		-2.71		461
LCB	267	371			-0.77		356	
LWS	262	372			-0.74		360	
CPP	277	368			-0.83		357	
LCB/PE (1:1)	260	307	378	469	-0.79	-0.55	297	416
LWS/PE (1:1)	277	384	384	494	-0.42	-0.75	349	460
CPP/PE (1:1)	282	374	374	495	-0.47	-0.71	342	465

Note: a the initial decomposition temperature of the first main pyrolysis stage; b the final decomposition temperature of the first main pyrolysis stage; c the initial decomposition temperature of the second main pyrolysis stage; d the final decomposition temperature of the second main pyrolysis stage; e the maximum weight loss rate of the first main pyrolysis stage; f the maximum weight loss rate of the second main pyrolysis stage; g the temperature of maximum weight loss rate of the first main pyrolysis stage; h the temperature of maximum weight loss rate of the second main pyrolysis stage; i not applicable.

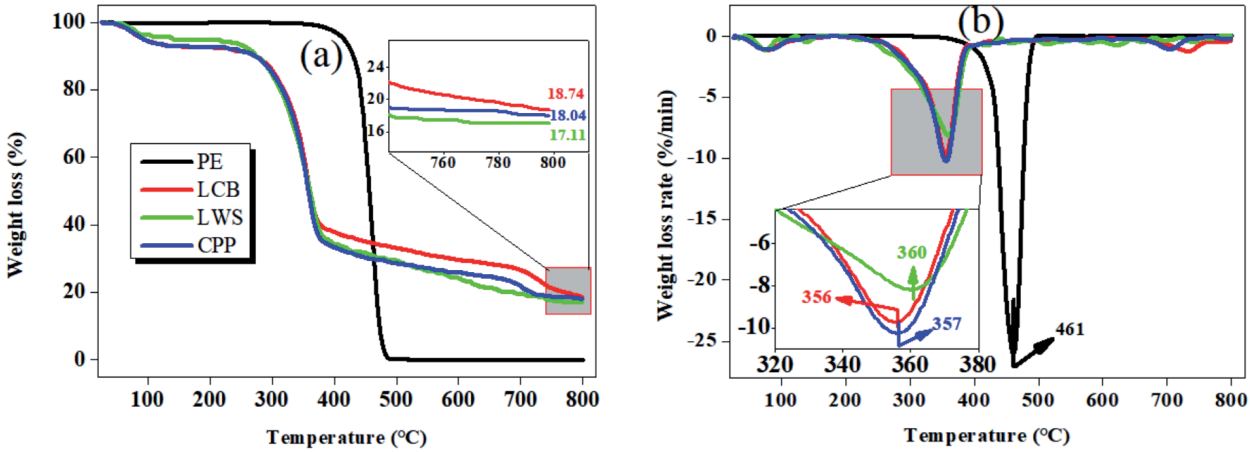

Fig. 6. Thermogravimetric analysis of packaging solid waste in the tobacco commercial cigarette logistics industry during pyrolysis; a) TG curves, b) DTG curves.

in biomass are approximately 220~380°C, 300~400°C, and 220~600°C, respectively. Based on this, it can be inferred that cellulose is the primary component in LCB, LWS, and CPP. Their maximum rates of mass loss are comparable, occurring at 35°C, 360°C, and 357°C, respectively (Fig. 6b)).

Co-pyrolysis

PE was individually blended with LCB, LWS, and CPP at mass ratios ranging from 5:1 to 1:5 and subsequently subjected to co-pyrolysis, and the pyrolysis behavior of the resulting mixtures was analyzed by thermogravimetric analysis (TGA). The TG curves indicate that the pyrolysis process of the mixtures can be divided into five stages: dehydration, pyrolysis preparation, a main pyrolysis stage attributed to LCB, LWS, or CPP in the mixture, a pyrolysis stage corresponding to PE, and carbonization (Fig. 7a)). For PE-LCB, the main pyrolysis interval associated with LCB is 260~307°C, which is slightly lower than that of LCB alone (267~371°C) (see Table 3). In contrast, the initial pyrolysis temperatures for the main decomposition stages assigned to LWS and CPP in the blends are 277°C and 282°C, respectively, both higher than those observed in the individual pyrolysis of LWS and CPP. According to previous studies, during co-pyrolysis, the softening of plastics at relatively lower temperatures may encapsulate biomass particles, thereby hindering the escape of volatile components and shifting the decomposition temperature of biomass in the mixture to higher values [11, 12]. This effect is confirmed in the results for PE-LWS and PE-CPP. Notably, PE-LCB exhibits the opposite behavior, which can be attributed to the presence of minerals or additives in LCB that may help mitigate the adverse effects of plastic softening during co-pyrolysis. On the other hand, compared to the individual pyrolysis of PE, the initial decomposition temperatures of PE in PE-LCB, PE-LWS, and PE-CPP decrease to 378°C, 384°C, and 374°C, respectively. This is mainly attributed to the formation of large amounts of oxygen-containing intermediates from the biomass (LCB, LWS, and CPP) during pyrolysis, which can disrupt the chemical bonds of PE and lower the activation energy required for its decomposition [20, 22]. The DTG curves show that the maximum mass loss rates for LCB and PE in PE-LCB occur at 297°C and 416°C, respectively, both of which are shifted to lower temperatures compared to the individual components. PE-LWS and PE-CPP mixtures exhibit similar trends, although the changes in thermal decomposition behavior, especially for PE, are less pronounced than those observed for the single components.

Interaction between PE and LCB, LWS, or CPP

To elucidate the interactions between the components during co-pyrolysis, the actual and theoretical mass changes of the mixtures during pyrolysis were calculated using Equation)1).

$$\Delta W = W_{mixture} - (x_1 W_1 + x_2 W_2) \quad (1)$$

where $W_{mixture}$ is the actual mass change of the mixture, W_1 and W_2 represent the mass changes of PE and the biomass (including LCB, LWS, or CPP) during individual pyrolysis, and x_1 and x_2 denote the mass fractions of PE and biomass in the mixture, respectively.

As shown in Fig. 8, when the pyrolysis temperature is below 260°C, the ΔW of PE-LCB fluctuates slightly, around ±2%. This is mainly because, at relatively low pyrolysis temperatures, PE and LCB may undergo phase transitions (such as softening or glass transition), but significant interactions are absent [23]. With further increases in pyrolysis temperature, the ΔW of PE-LCB declines rapidly and reaches a minimum

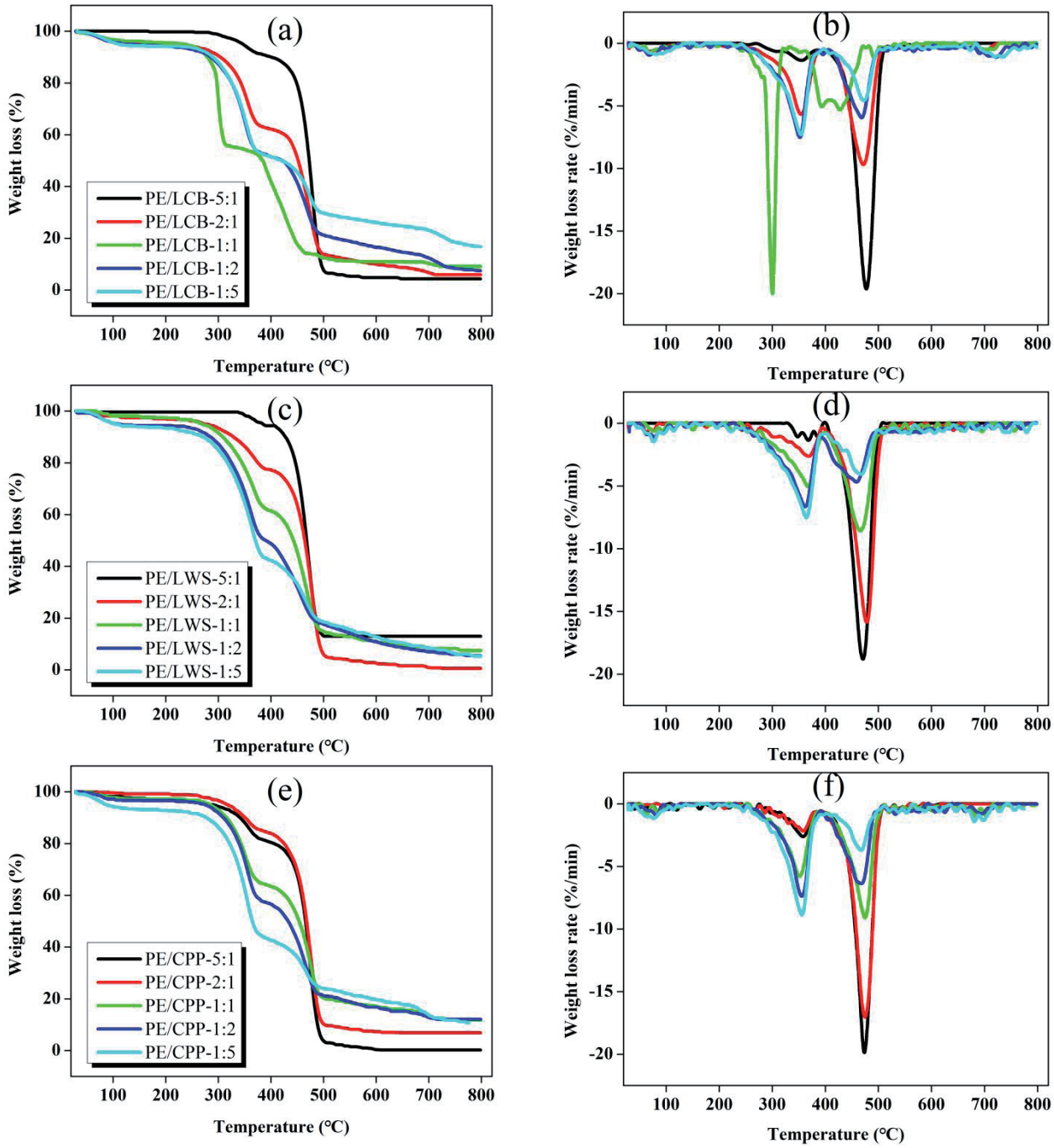

Fig. 7. Thermogravimetric analysis of packaging solid waste in the tobacco commercial cigarette logistics industry during co-pyrolysis; a) TG curves, b) DTG curves.

of -38.53% at 438°C. This indicates that, within this temperature range, the actual mass loss rate of PE-LCB is significantly higher than the theoretical value, suggesting strong interactions between PE and LCB. Based on previous analyses, this is primarily attributed to the reinforcing effect of minerals or additives in LCB on the interaction between the two components [11]. When the pyrolysis temperature exceeds 438°C, the ΔW of PE-LCB increases rapidly. Within the 480-800°C interval, it changes slowly and gradually approaches zero, indicating that a certain degree of synergistic effect between PE and LCB remains in the carbonization stage. On the other hand, PE-LWS and PE-CPP display similar trends in ΔW. At lower pyrolysis temperatures (<328°C), the interaction between PE and LWS or CPP is weak, resulting in only minor effects on the mass change of the mixtures. As the temperature increases, the ΔW of PE-LWS and PE-CPP first slightly decreases and then increases sharply, reaching their respective maxima of 6.31% and 16.40% at 470°C and 472°C, where the inhibitory effect of PE on the pyrolysis of LWS or CPP is most pronounced. Subsequently, the ΔW of both

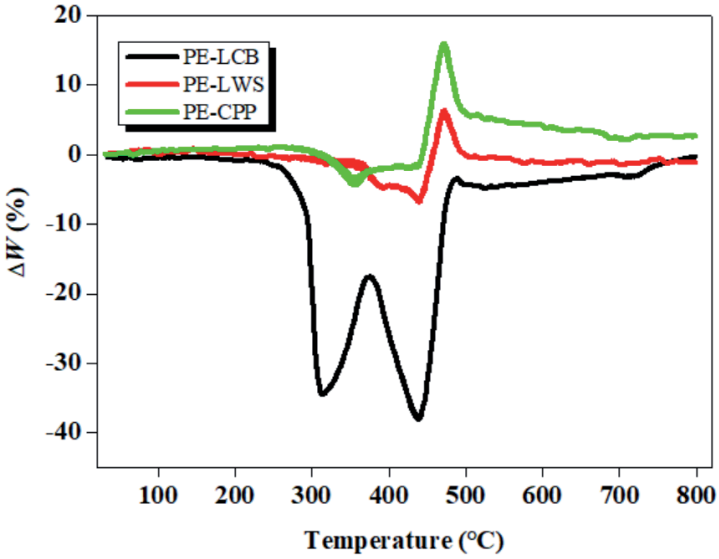

Fig. 8. Variation of ΔW for samples.

PE-LWS and PE-CPP gradually declines, further indicating that there is still some degree of interaction between PE and LWS or CPP during the carbonization stage.

Kinetic Analysis

To quantitatively analyze the pyrolysis characteristics of PE, LCB, LWS, CPP, and their mixtures, the activation energy (*E*) and pre-exponential factor (*A*)

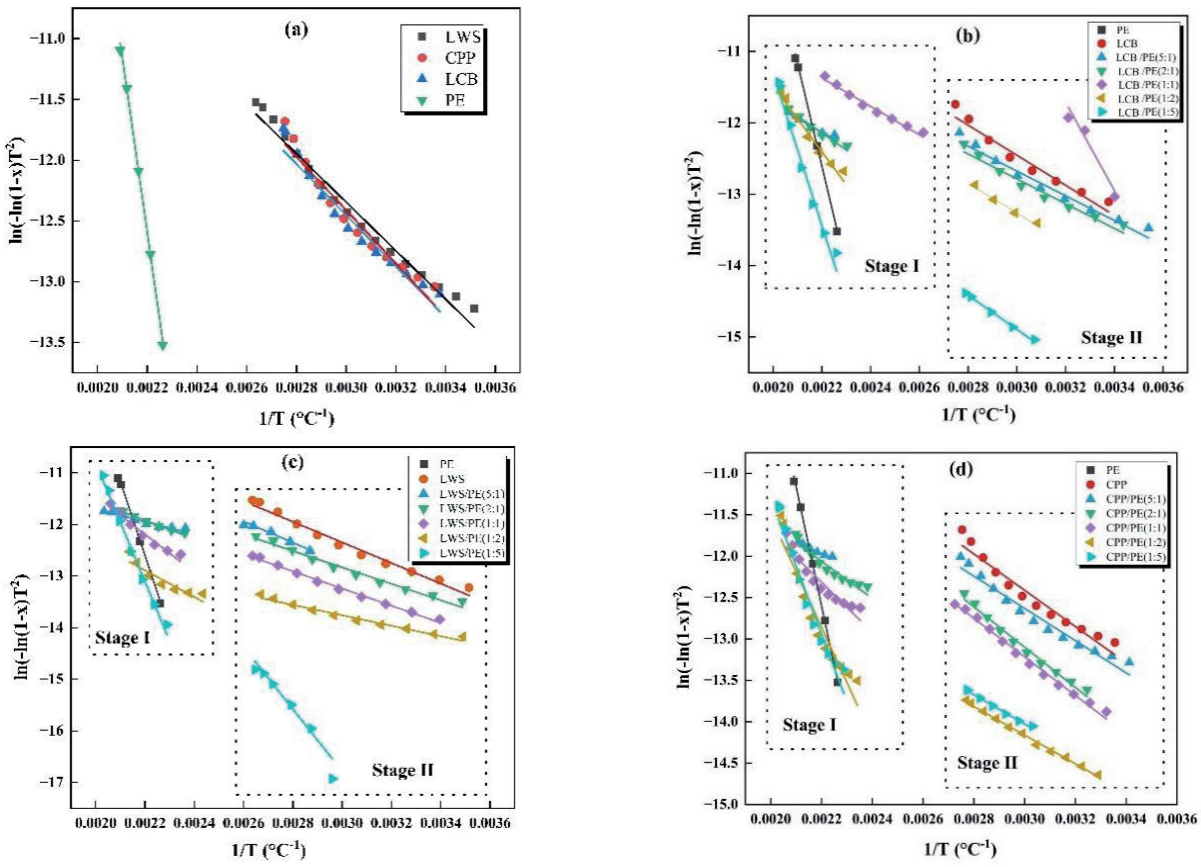

Fig. 9. First-order kinetic fitting of the pyrolysis process; a) individual components, b) mixtures of LCB and PE at different ratios, c) mixtures of LWS and PE at different ratios, d) mixtures of CPP and PE at different ratios.

Table 4. Kinetic analysis parameters of samples during pyrolysis/co-pyrolysis.

	Temperature Range (°C)	*x* (%)	E (kJ/mol)	A (min^{-1})	R^2
PE	407~485	92.58	119.53	2.67E+10	0.99
LCB	267~371	58.59	17.51	4.55E-02	0.96
LWS	262~372	50.79	16.61	3.46E-02	0.98
CPP	277~368	57.88	18.24	6.43E-02	0.97
LCB/PE (1:1)	260~307	26.78	11.41	2.00E+05	0.97
	378~465	33.48	16.53	1.81E-02	0.96
LWS/PE (1:1)	277~384	29.85	18.84	4.35E-03	0.98
	384~494	40.32	30.47	5.91E-01	0.96
CPP/PE (1:1)	282~374	26.33	19.36	4.58E-02	0.96
	374~495	36.88	25.17	1.06E-01	0.92

during pyrolysis were calculated using the Arrhenius Equation combined with a first-order kinetic model [21].

$$\frac{dx}{dt} = A\exp[(\frac{-E}{RT})(1-x)] \quad (2)$$

Where E is the activation energy (kJ/mol); A is the pre-exponential factor (min^{-1}); T is the temperature (K); R is the universal gas constant; and x represents the conversion rate.

As shown in Fig. 9 and Table 4, the correlation coefficients (R^2) for fitting the pyrolysis behaviors of PE, LCB, LWS, CPP, and their mixtures using the first-order kinetic model are between 0.92 and 0.99, indicating that the first-order kinetic model can well describe these reaction processes, consistent with previous reports [12]. The pyrolysis of single-component PE, LCB, LWS, and CPP can be described by a single first-order kinetic model, while the thermal decomposition of their mixtures can be fitted using two consecutive first-order kinetic models. The first stage and the second stage represent the decomposition of biomass components (LCB, LWS, or CPP) and PE, respectively. The activation energy (E) of PE is 119.53 kJ/mol, which is 6.6-7.2 times higher than that of LCB, LWS, and CPP. The higher activation energy of PE is associated with its relatively high thermal stability (see Fig. 6). When PE is co-pyrolyzed with LCB (i.e., PE-LCB), the activation energy of LCB in the mixture decreases by more than 30% compared to that of pure LCB. As discussed above, this is mainly related to the promotive effects of minerals or additives present in LCB on the pyrolysis process. In the cases of PE-LWS and PE-CPP, the activation energies of the biomass components (LWS and CPP) in the mixtures increase slightly, primarily due to the encapsulating effect of softened plastics. Notably, in all mixtures, the activation energy of PE is significantly reduced compared to that of pure PE, which can be attributed to the destruction of PE chemical bonds by oxygenated intermediates released during the pyrolysis of biomass.

Conclusions

PE contains a high proportion of carbon (84.39%) and hydrogen (13.58%), along with a small amount of oxygen (1.63%). FT-IR and SEM analyses revealed that the predominant surface functional groups of PE are C-H and -OH, and its surface exhibits a smooth and flat morphology. In contrast, LCB, LWS, and CPP are not only rich in C, H, and O, but also contain measurable amounts of N and S. Their surface functional groups include C=O, -C-O, C-H, and -OH. SEM observations showed that LCB, LWS, and CPP all possess fibrous structures, with a large number of mineral particles or additives distributed on their surfaces. Thermogravimetric analysis of the individual components indicated that PE exhibits relatively high thermal stability, decomposing over a narrow temperature range (407~485°C) and leaving negligible solid residue after pyrolysis. The pyrolysis processes of LCB, LWS, and CPP are more complex, generally comprising four stages: dehydration, pyrolysis preparation, main pyrolysis, and carbonization. During co-pyrolysis, strong interactions were observed between PE and LCB, LWS, or CPP. Notably, for PE/LCB blends, the minerals or additives in LCB significantly mitigated the adverse effects caused by the softening of PE, resulting in a shift of the pyrolysis temperatures of both LCB and PE towards lower values and an obvious reduction in their activation energies.

Acknowledgments

This work was supported by the Key Research and Development Program of Guizhou Branch Company of China Tobacco Cooperation (2023XM24,

2023XM11, and 2023XM17), the National Natural Science Foundation of China (52260018, 42263007, and 42167067), the Scientific Research Fund of Guizhou Minzu University (GZMUZK[2023]CXTD03), and the Department of Education of Guizhou Province (No. QianJiaoJi[2023]034).

Conflict of Interests

The authors declare that they have no known competing financial interests or personal relationships that could have appeared to influence the work reported in this paper.

References

1. ZHANG Y., YANG S.W., ZHANG H. Relationship between the scale, structure, efficiency and economic growth of tobacco financial development in China. Tobacco Regulatory Science, **7**, 432, **2021**.
2. REN T.B., YAN D., ZHANG Y.J., LI X.Y., CHEN J., WANG C.L., WANG C., LI P.Y., WANG L.F., ZENG Q., CAI X.J. Biomass moulding fuel for zero-emission agricultural waste management: A case study of tobacco curing in China. Journal of Environmental Management, **377**, 124612, **2025**.
3. SHEN X.P., ZHANG Y.H., TANG Y.M., QIN Y.F., LIU N., YI Z.L. A study on the impact of digital tobacco logistics on tobacco supply chain performance: taking the tobacco industry in Guangxi as an example. Industrial Management & Data Systems, **122**, 1416, **2022**.
4. KUMAR A., SAMADDER S.R. A review on technological options of waste to energy for effective management of municipal solid waste. Waste Management, **69**, 407, **2017**.
5. LEE D.J., LU J.S., CHANG J.S. Pyrolysis synergy of municipal solid waste (MSW): A review. Bioresource Technology, **318**, 123912, **2020**.
6. LU J.S., CHANG Y.J., POON C.S., LEE D.J. Slow pyrolysis of municipal solid waste (MSW): A review. Bioresource Technology, **312**, 123615, **2020**.
7. DU Y.F., JU T.Y., MENG Y., LAN T., HAN S.Y., JIANG J.G. A review on municipal solid waste pyrolysis of different composition for gas production. Fuel Processing Technology, **224**, 107026, **2021**.
8. WANG Z.W., BURRA K.G., LEI T.Z., GUPTA A.K. Co-pyrolysis of waste plastic and solid biomass for synergistic production of biofuels and chemicals-A review. Progress in Energy and Combustion Science, **84**, 100899, **2021**.
9. TEE M.Y., WOON K.S., WONG S.L., NYAKUMA B.B., TAN J.P., CHONG W.W.F., MONG G.R. Unveiling the dynamics of solid waste co-pyrolysis through thermogravimetric analysis and kinetic analysis for technological upscaling (2001-2022). Journal of Analytical and Applied Pyrolysis, **183**, 106806, **2024**.
10. ESSO S.B.E., ZHE X., CHAIWAT W., KAMARA M.F., XU L.F., JUN X., EBAKO J., LONG J., SHENG S., SONG H., YI W., JUN X. Review on synergistic effects during co-pyrolysis of biomass and plastic waste: Significance of operating conditions and interaction mechanism. Biomass & Bioenergy, **159**,106415, **2022**.
11. WANG Z., SHEN D., WU C., GU S. Thermal behavior and kinetics of co-pyrolysis of cellulose and polyethylene with the addition of transition metals. Energy Conversion and Management, **172**, 32, **2018**.
12. WANG Z.H., LIU G.F., SHEN D.K., WU C.F., GU S. Co-pyrolysis of lignin and polyethylene with the addition of transition metals - Part I: Thermal behavior and kinetics analysis. Journal of the Energy Institute, **93**, 281, **2020**.
13. WU X.K., GUO T., CHEN Z.Y., WANG Z.H., QIN K., WANG Z.K., AO Z.Q., YANG C., SHEN D.K., WU C.F. Facile and green preparation of solid carbon nanoonions via catalytic co-pyrolysis of lignin and polyethylene and their adsorption capability towards Cu(ii). RSC Advances, **12**, 5042, **2022**.
14. WANG X.X., DAI Y.W., LIU J.Q., ZHANG A.L., TAO K.P., DAI B., ZHOU S.Z., KONG L.T., LIU J.C., LI J.B. Ultrathin ZSM-5: a catalyst for efficient aromatics synthesis in the co-pyrolysis of cotton stalk and polyethylene. Fuel, **401**, 135839, **2025**.
15. GUAN X.Y., DAI Y.M., LI X., HAN Z.Y., LI X., SU Z.C., WANG X.J., WANG L., XU M.K. Acetochlor promotes the aging of mulch-derived microplastics in soil by altering the plastisphere microbial community. Journal of Hazardous Materials, **494**, 138641, **2025**.
16. QIN K., WANG Z.H., ZHANG H.Y. Evolution of surface functional groups in the pyrolysis of lignin with the introduction of polyethylene and transition metals. CIESC Journal, **73**, 5201, **2022**.
17. IKBARIEH A., DAI S.C. Compressibility and permeability of particulated non-recyclable municipal solid waste. Waste Management, **201**, 114809, **2025**.
18. ESFANDIARI Z., HASSANI B., SANI I.K., TALEBI A., MOHAMMADI F., ZOMORODI S., KAVEH M., ASSADPOUR E., KHODAEI S.M., EGHBALJOO H., GHOLIZADEN H., SANI M.A., JAFARI S.M. Characterization of edible films made with plant carbohydrates for food packaging: A comprehensive review. Carbohydrate Polymer Technologies and Applications, **11**, 100979, **2025**.
19. SONG G.J., AZAD S.A., HU W.H., MADADI M., RAHMAN A., SUN C.H., SUN F.B. Comparison study and mechanisms insight of $AlCl_3$-catalyzed different organosolv pretreatment of lignocellulose: Enhancing enzymatic hydrolysis, lignin fractionation, and furfural production. Bioresource Technology, **439**, 133308, **2026**.
20. BU Q., CHEN K., XIE W., LIU Y., GAO M., KONG X., CHU Q., MAO H. Hydrocarbon rich bio-oil production, thermal behavior analysis and kinetic study of microwave-assisted co-pyrolysis of microwave-torrefied lignin with low density polyethylene. Bioresource Technology, **291**, 121860, **2019**.
21. JIN Q., WANG X., LI S., MIKULCIC H., BESENIC T., DENG S., VUJANOVIC M., TAN H., KUMFER B.M. Synergistic effects during co-pyrolysis of biomass and plastic: Gas, tar, soot, char products and thermogravimetric study. Journal of the Energy Institute, **92**, 108, **2019**.
22. XIANG Z., LIANG J., MORGAN H.M., LIU Y., MAO H., BU Q. Thermal behavior and kinetic study for co-pyrolysis of lignocellulosic biomass with polyethylene over Cobalt modified ZSM-5 catalyst by thermogravimetric analysis. Bioresource Technology, **247**, 804, **2018**.
23. KAI X.P., YAN W.W., YANG T.H., ZHANG T., LI B.S., LIU Z.W., WANG L.S., LI R.D. Study on co-pyrolysis of enzymolytic lignin and high-density polyethylene: Effects of pyrolysis parameters and synergistic interactions on the product distribution and characteristics. Journal of the Energy Institute, **123**, 102209, **2025**.